Electronic Supplementary Information (ESI)

Heterostructured Electrocatalyst for the Electrocatalytic Valorization of 5-Hydroxymethylfurfural Coupled with Hydrogen Evolution Reaction

Loknath Thapa[a#], Asim Bhaumik[b], Swastik Mondal[c,d], and C. Retna Raj[a*]

[a] *Functional Materials and Electrochemistry Lab, Department of Chemistry IIT Kharagpur, Kharagpur-721302, West Bengal, India*
E-mail: crraj@chem.iitkgp.ac.in
[#]Main contributor

[b] *School of Material Sciences, Indian Association for the Cultivation of Science, Kolkata 700032, West Bengal, India*

[c] *CSIR–Central Glass and Ceramic Research Institute,196 Raja S C Mullick Road, 700 032, Kolkata, India*
[d]*Academy of Scientific and Innovative Research (AcSIR), Ghaziabad–201002, India*

Synthesis of Ni_9S_8

Ni_9S_8 was synthesized by annealing the mixture of $NiCl_2 \cdot 6H_2O$ (100 mg), $C_3N_6H_6$ (250 mg), and CH_4N_2S (250 mg) at the identical condition used for the synthesis of the ternary heterostructure (750 ^oC for 1 h under Ar atmosphere).

Synthesis of MoS_2

MoS_2 was synthesized by annealing $Na_2MoO_4 \cdot 2H_2O$ (100 mg) in presence of CH_4N_2S (250 mg) at the identical condition used for the synthesis of the ternary heterostructure.

Synthesis of MoC

MoC was synthesized by annealing the mixture of $Na_2MoO_4 \cdot 2H_2O$ (100 mg) and $C_3N_6H_6$ (250 mg) at the identical condition used for the synthesis of the ternary heterostructure.

Synthesis of FeP@NPC

It was synthesized according to procedure established in our lab using $[Fe(bpy)_3](PF_6)_2$ and melamine.[1]

Fig. S1 HPLC profile of HMF and FDCA and the corresponding calibration plots.

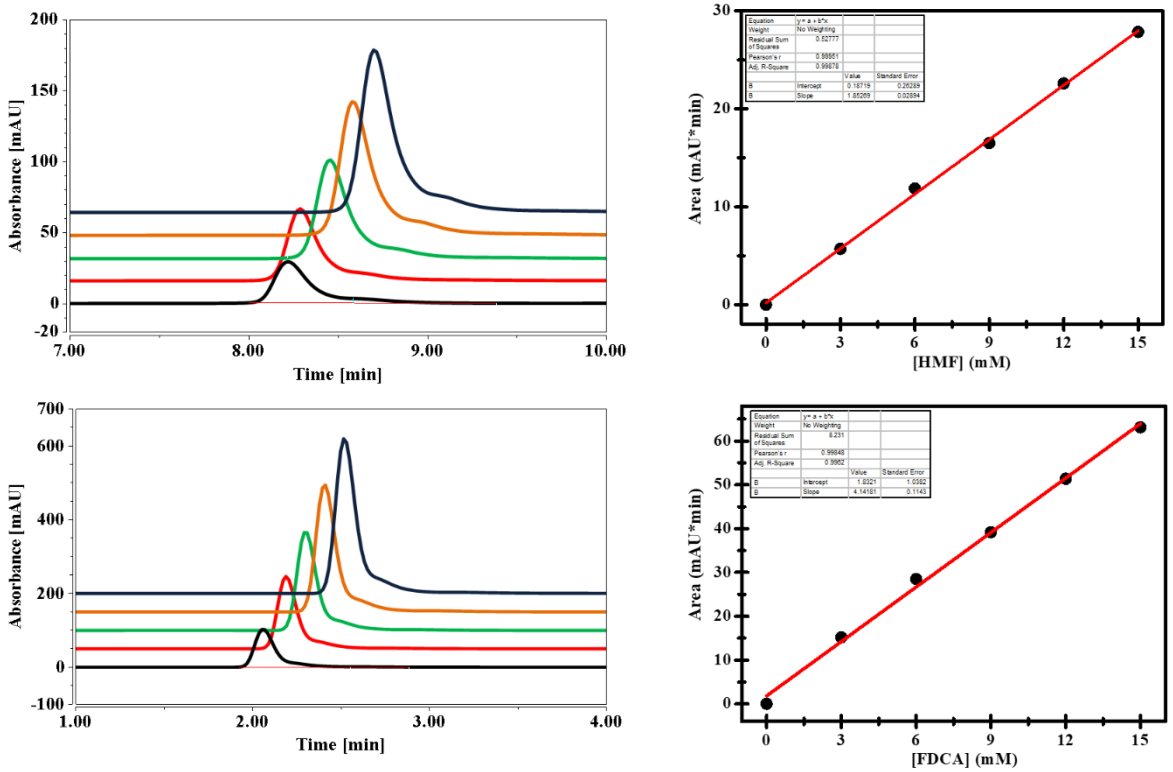

Fig. S2 HPLC profile of HMFCA and FFCA and the corresponding calibration plots.

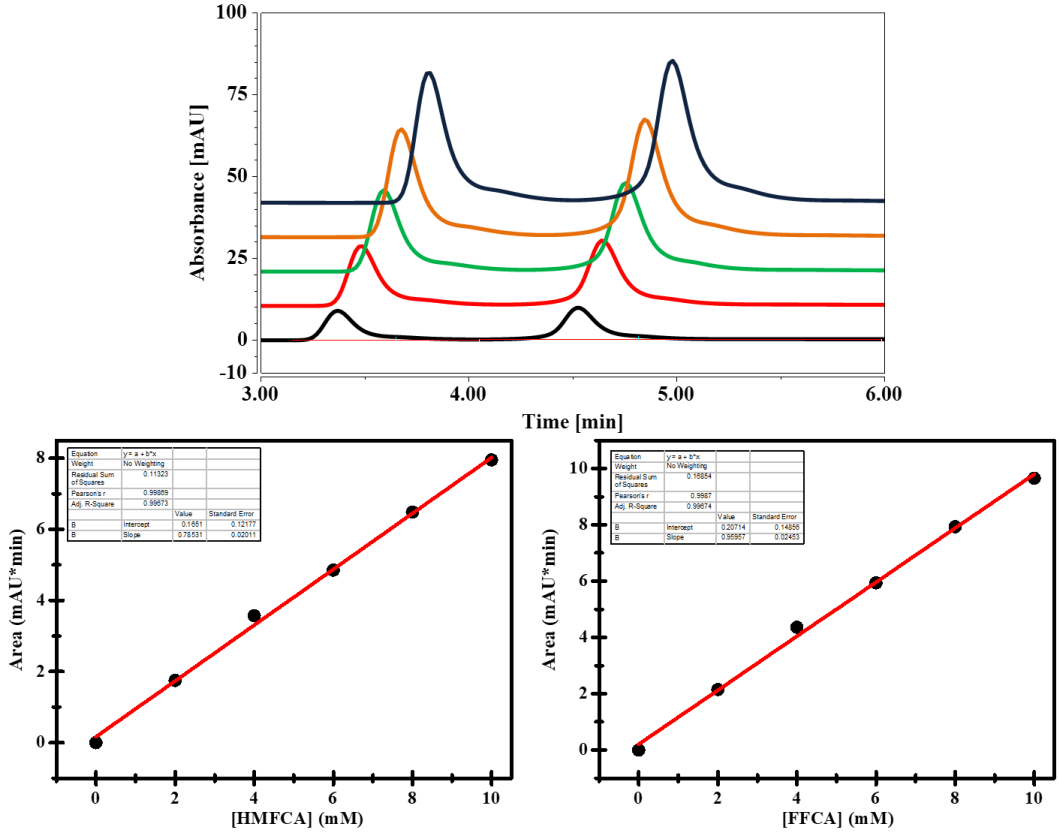

Fig. S3 XRD profile of the ternary heterostructure. Le Bail refinements (GOF = 1.23, Rp = 2.56, wRp = 3.24) confirms the presence of MoS_2, MoC, Ni_9S_8 and Ni_3S_2 phases.

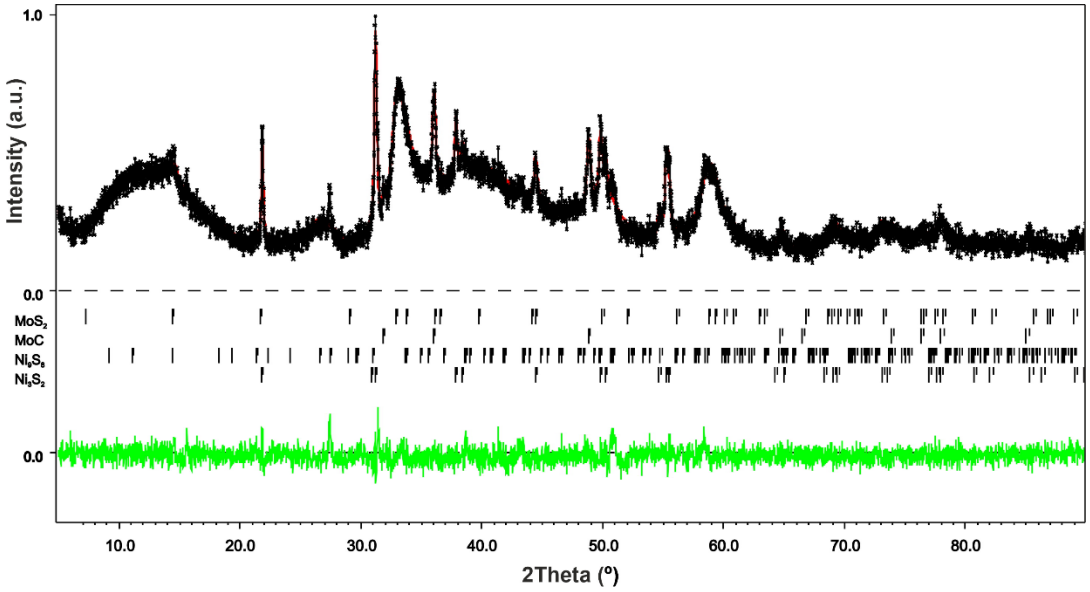

Fig. S4 FESEM images of $NiMoO_4$ nanowire bundle at different magnification.

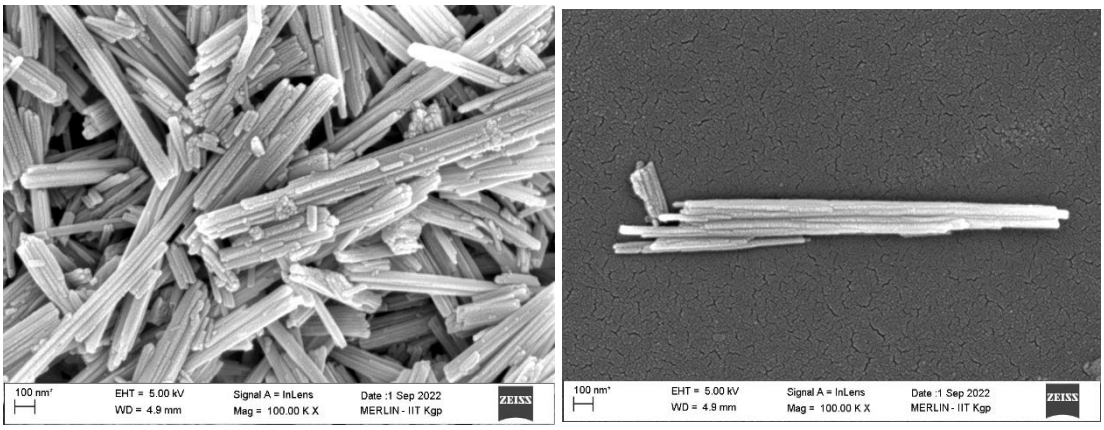

Fig. S5 (a) XRD profile, (b) FESEM image, and (c) EDX elemental mapping images of Ni_9S_8.

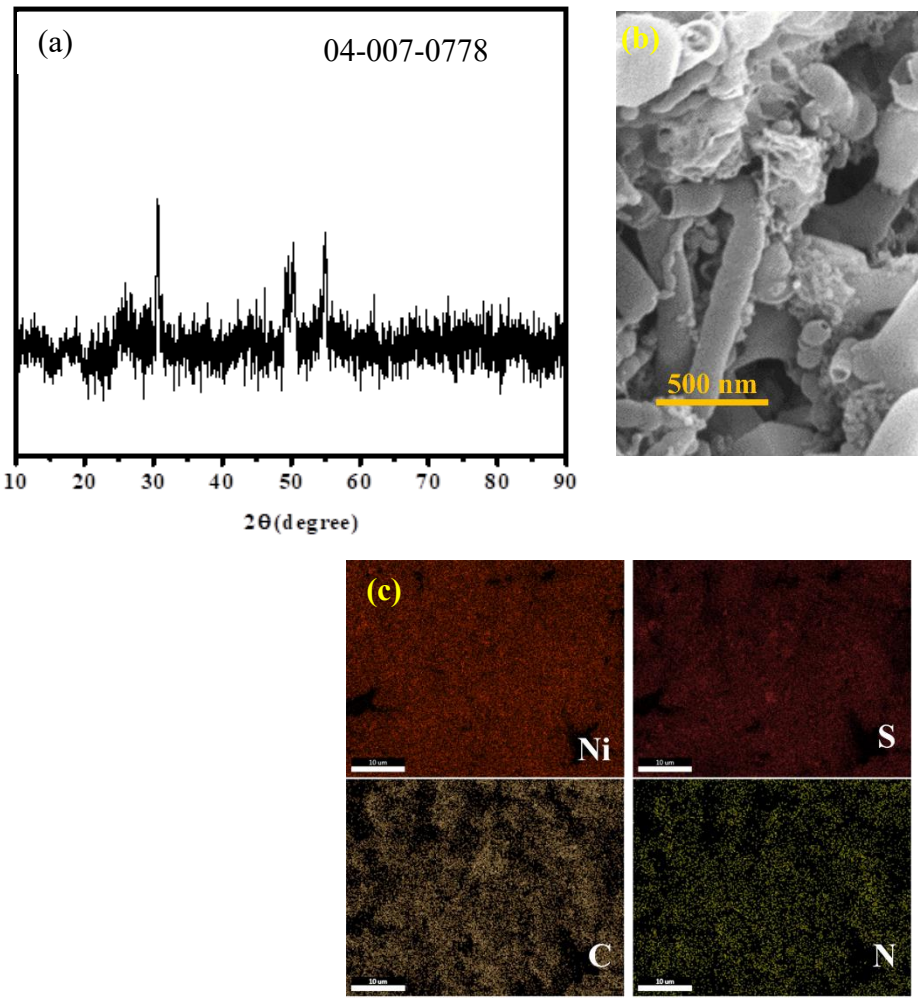

Fig. S6 (a) XRD profile, (b) FESEM image, and (c) EDX elemental mapping images of MoS_2.

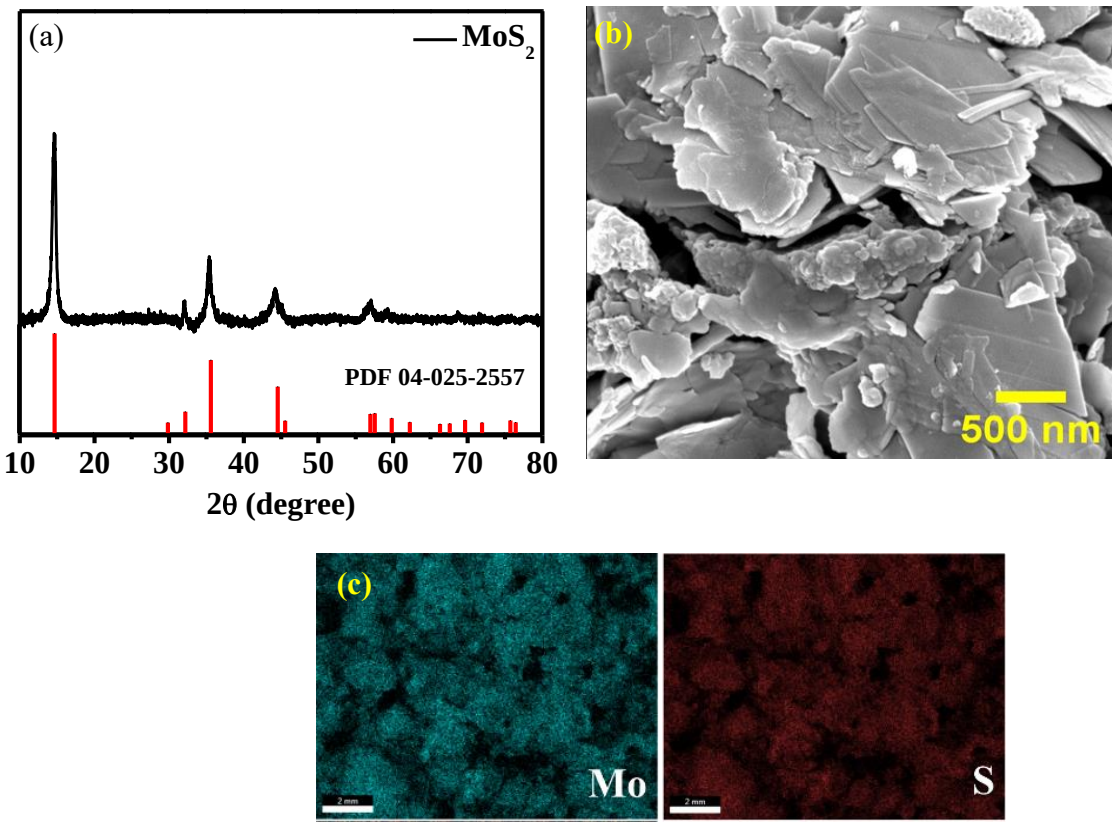

Fig. S7 (a) XRD profile, (b) FESEM image, and (c) EDX elemental mapping images of MoC.

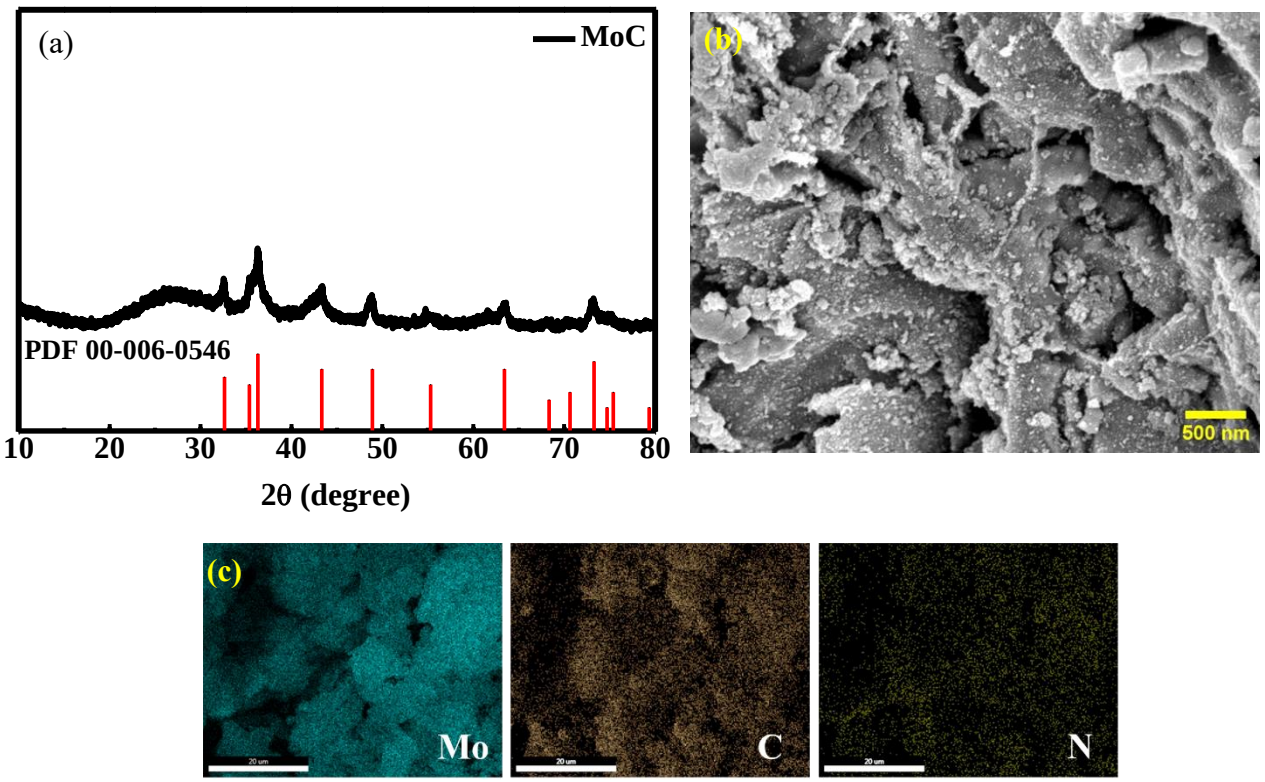

Fig. S8 TEM image depicting the presence of defects in MoS_2 sheets of $Ni_xS_y/MoS_2/MoC$ heterostructure. Low (a) and high resolution (b) images along with the inverse FFT images (1 to 3) are shown.

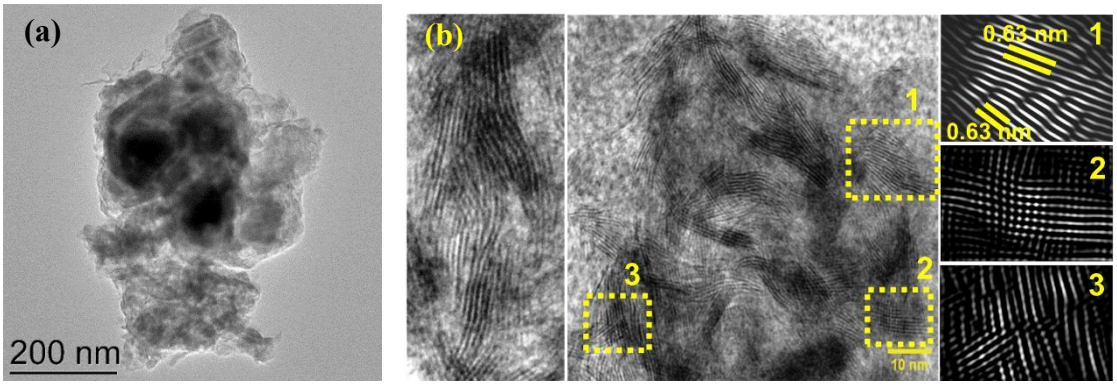

Fig. S9 (a) XPS survey scan, (b) N 1s spectra of $Ni_xS_y/MoS_2/MoC$ heterostructure.

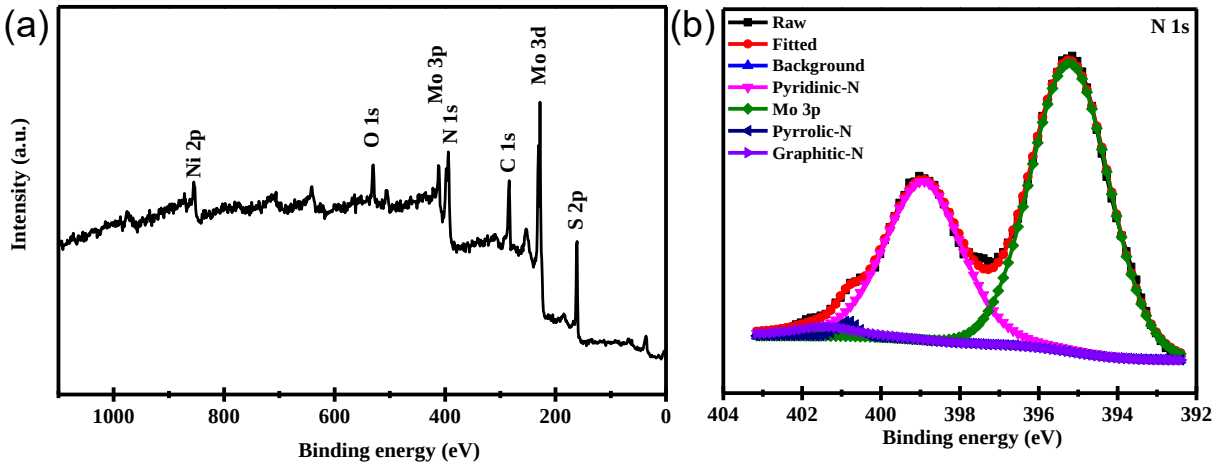

Fig. S10 N_2 adsorption/desorption isotherm of $Ni_xS_y/MoS_2/MoC$ heterostructure.

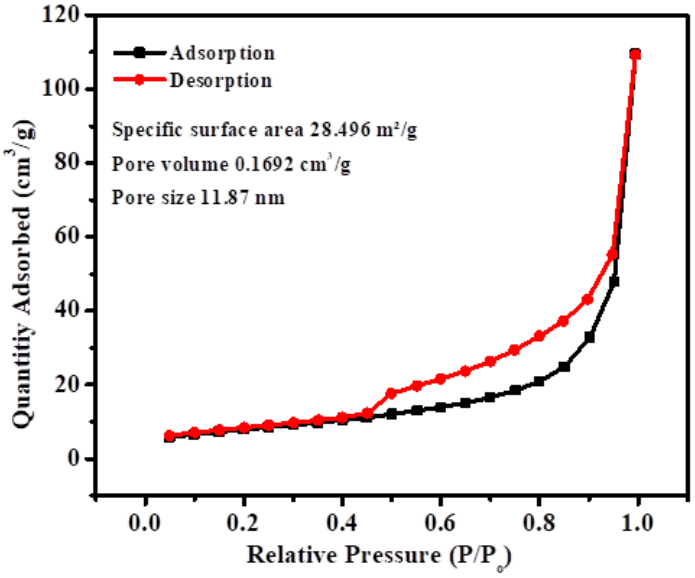

Fig. S11 Cyclic voltammetric profile of (a) $Ni_xS_y/MoS_2/MoC$ heterostructure and (b) Ni_9S_8 and the corresponding C_{dl} plot (c).

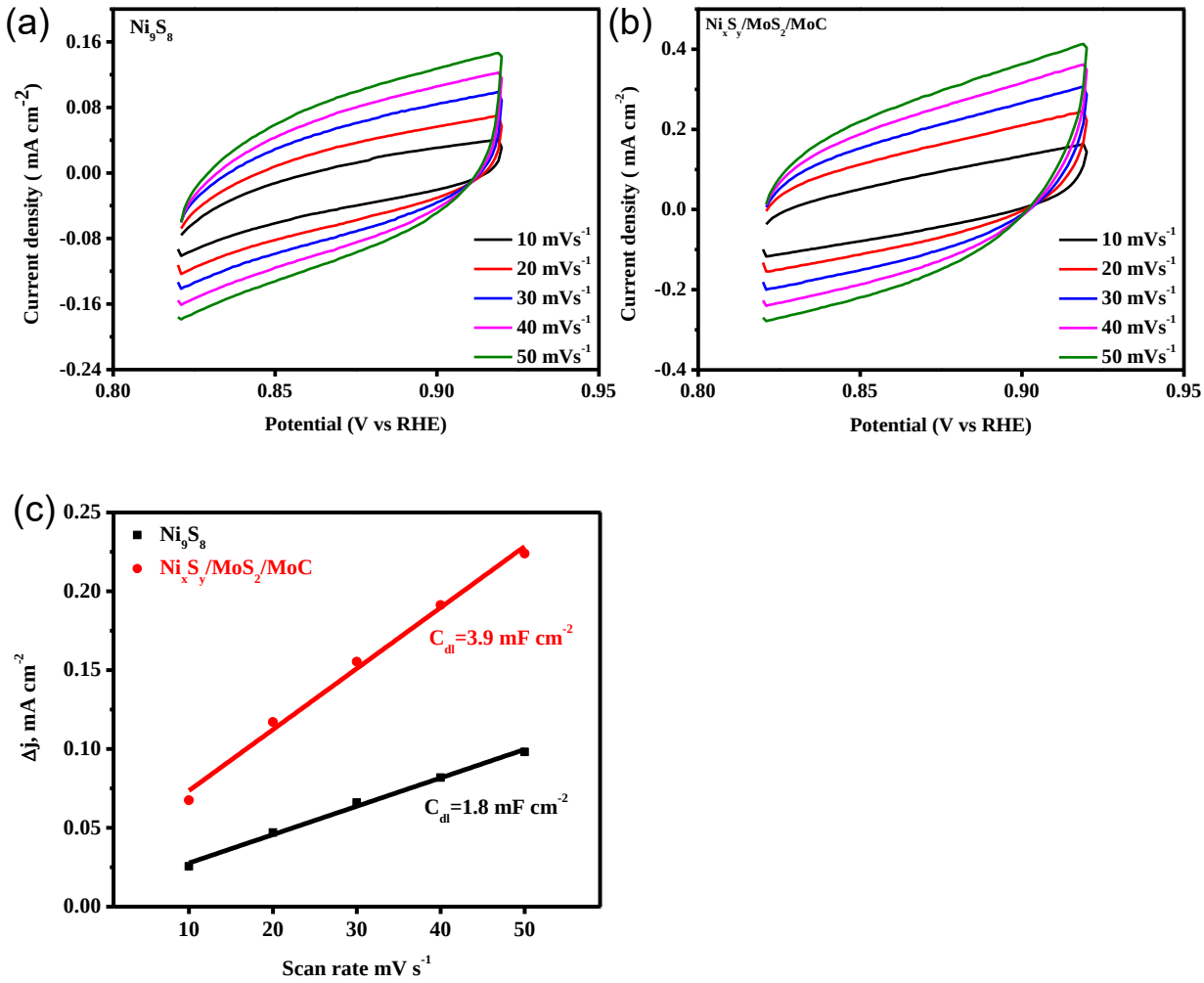

Fig. S12 Schematic illustration of the electrochemical cell used for HMF oxidation.

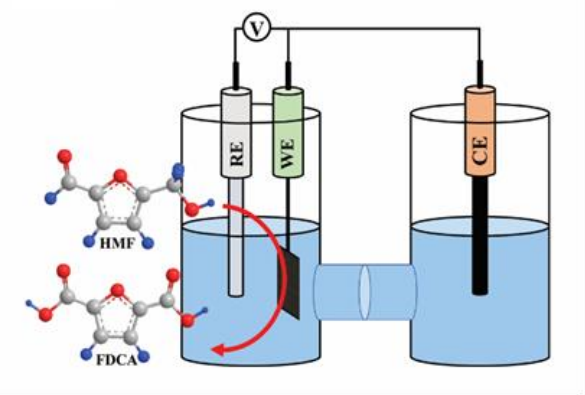

Fig. S13 Charge associated with the $Ni^{2+} \rightarrow Ni^{3+}$ redox reaction of (a) $Ni_xS_y/MoS_2/MoC$ heterostructure, (b) Ni_9S_8, (c) MoS_2/Ni_9S_8, and (d) MoC/Ni_9S_8. Charge was calculated by integrating the area under the background subtracted LSV. Sweep rate: 5 mV/s

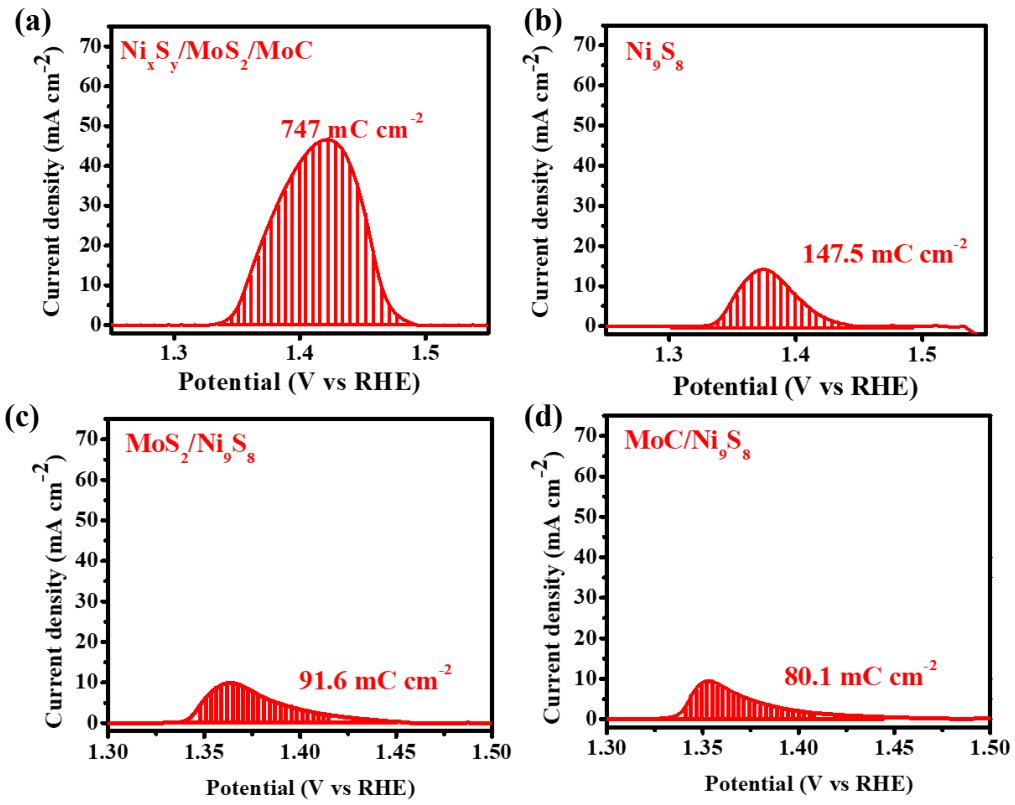

Fig. S14 (a) LSV of $Ni_xS_y/MoS_2/MoC$ in presence of 10 mM HMF with and without iR correction. Sweep rate: 5 mV/s

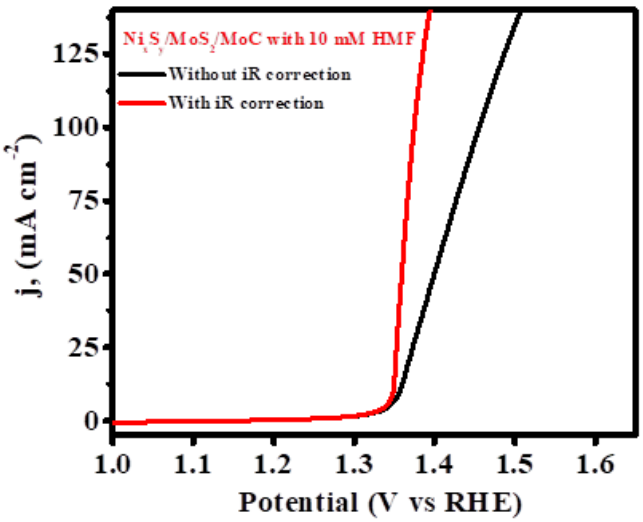

Fig. S15 LSV illustrating the activity of Ni_9S_8 towards HMF oxidation. Sweep rate: 5 mV/s

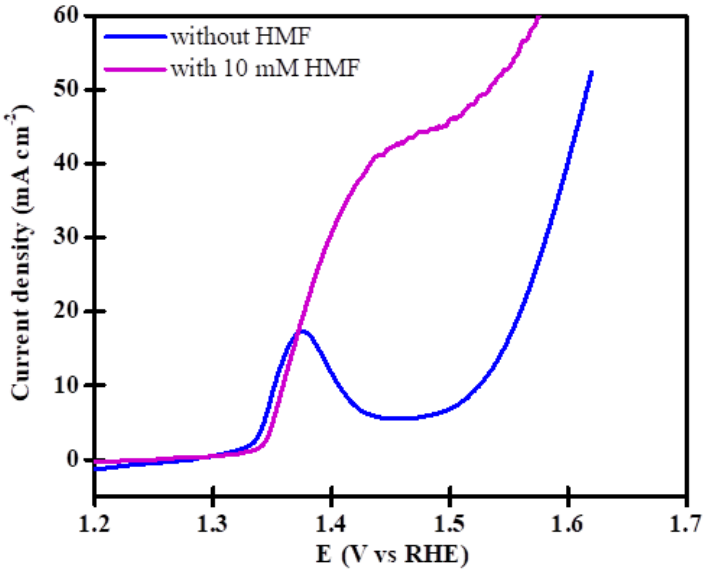

Fig. S16 LSV illustrating the catalytic activity of (a) MoC, (b) MoS_2, and binary (c) MoS_2/Ni_9S_8, and (d) MoC/Ni_9S_8 catalysts towards HMF oxidation. Sweep rate: 5 mV s^{-1}

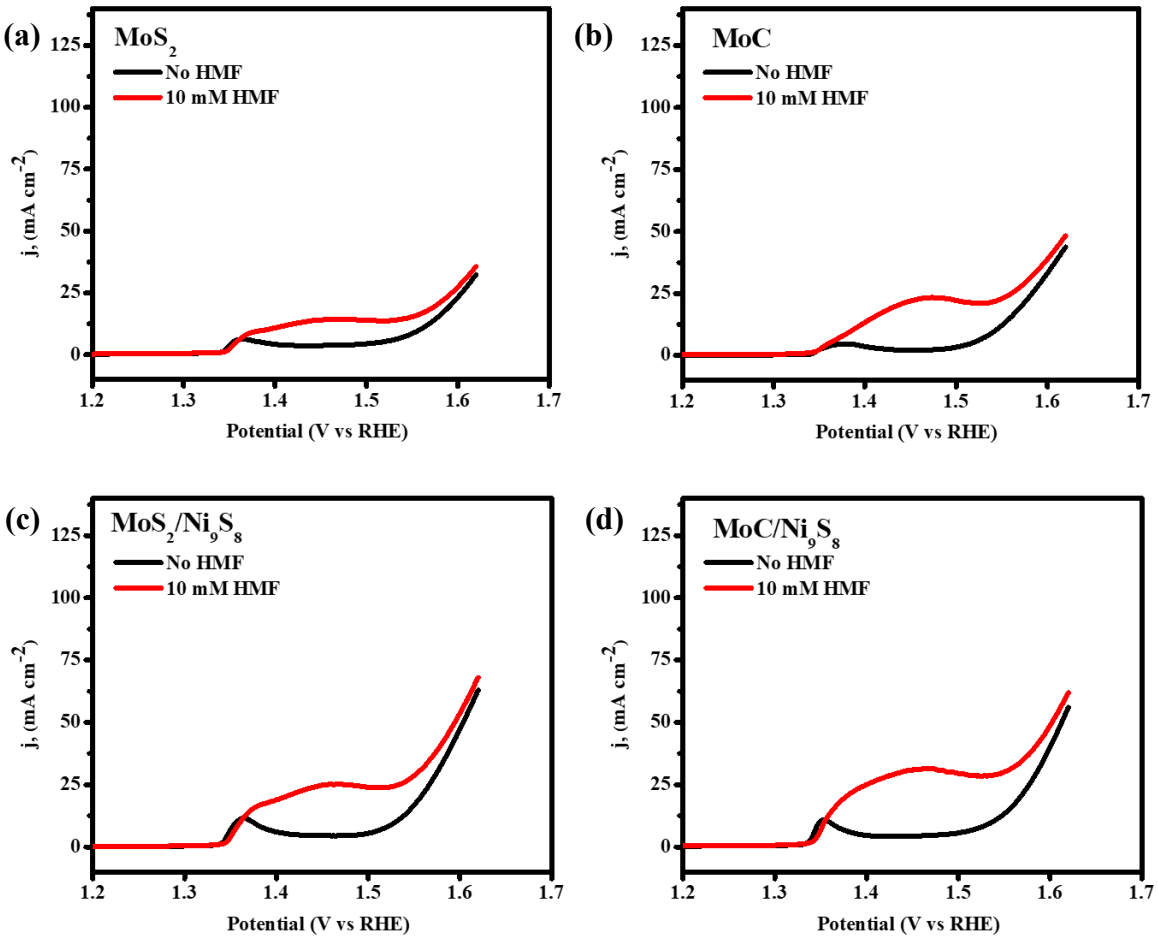

Fig. S17 Tafel plot of (a) $Ni_xS_y/MoS_2/MoC$ heterostructure and (b) Ni_9S_8.

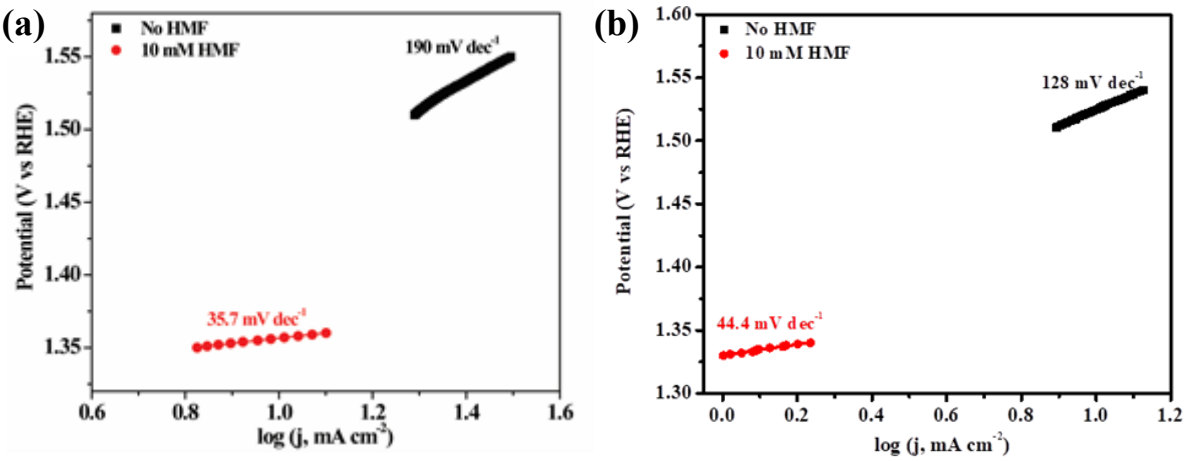

Fig. S18 ^{1}H-NMR of FDCA obtained from the anodic compartment (after acidification) (Inset photograph). Signals **a** and **b** are from the NMR solvent (methanol).

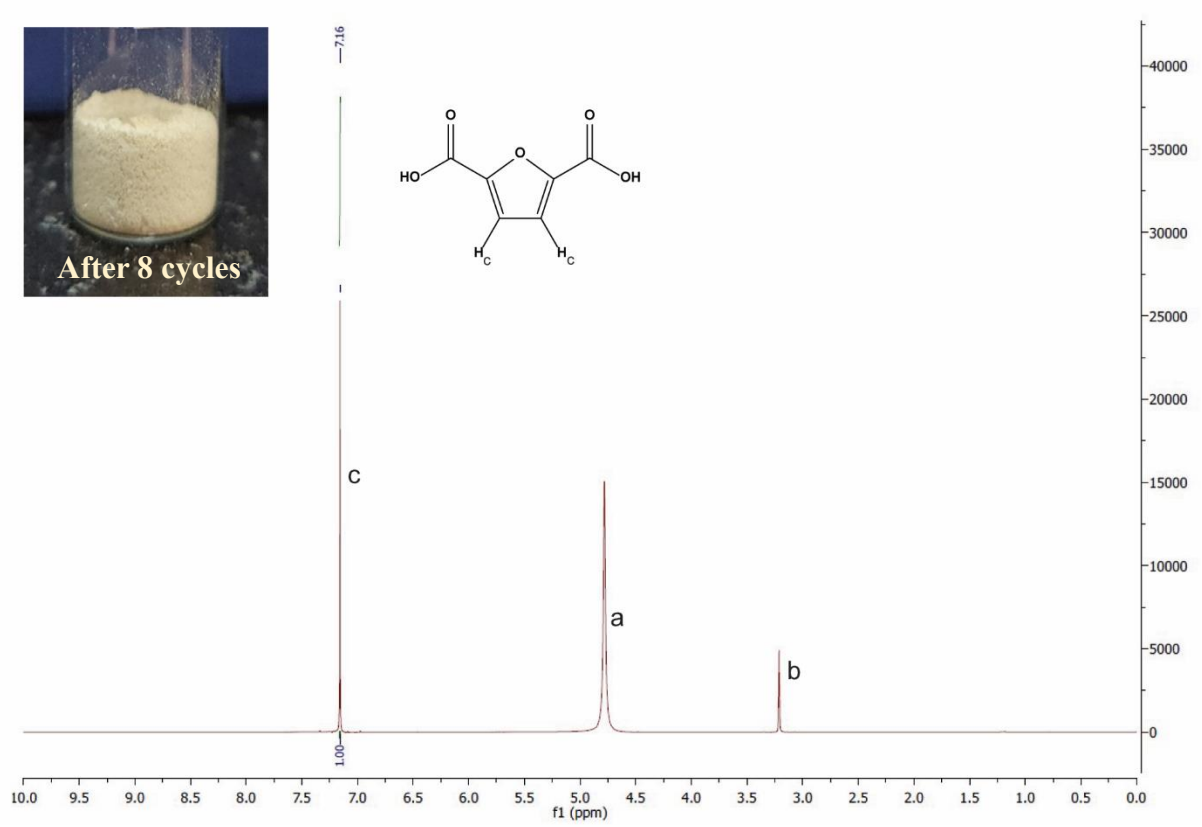

Fig. S19 (a, c) Current-time and charge-time transients obtained during constant potential electrolysis at 1.45 and 1.5 V, (b, e) HPLC profile, and (c, f) concentration vs charge plot for HMF, FDCA and the corresponding intermediates. These experiments were performed with electrode area of 1 cm^2 to avoid the current overflow.

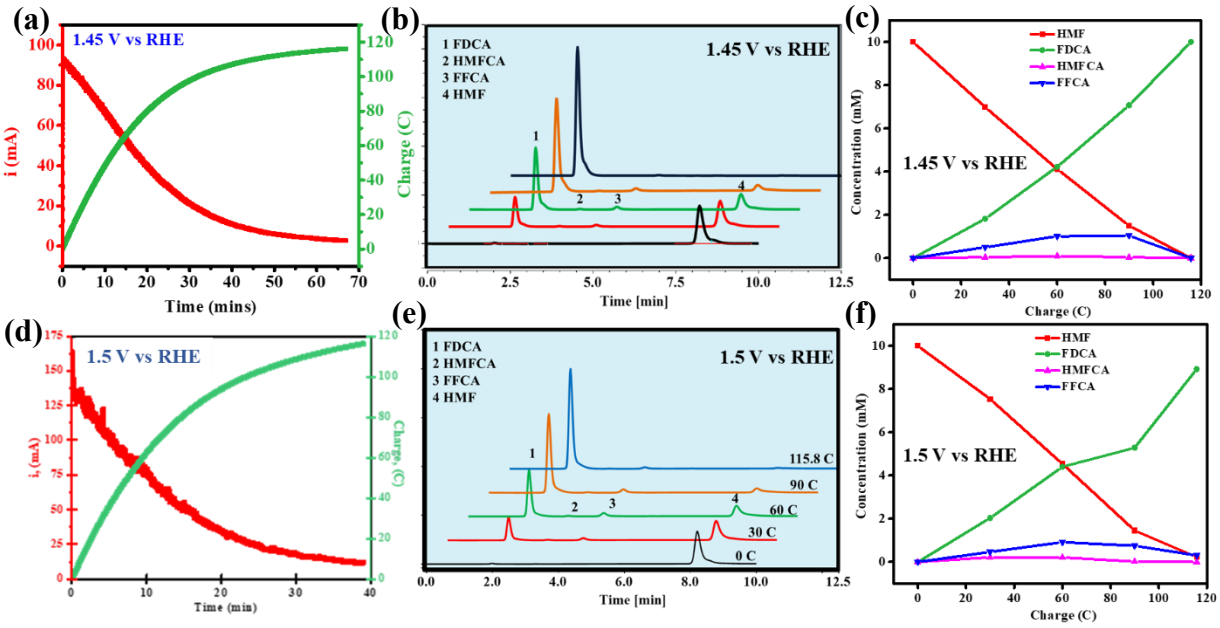

Fig. S20 (a-c) Current- and charge-time transients obtained during constant potential electrolysis at different potentials, (d-f) HPLC profile, and (g-i) concentration vs charge plot of HMF, FDCA and the corresponding intermediates at different charge passed interval during the electrolysis using Ni_9S_8 catalyst.

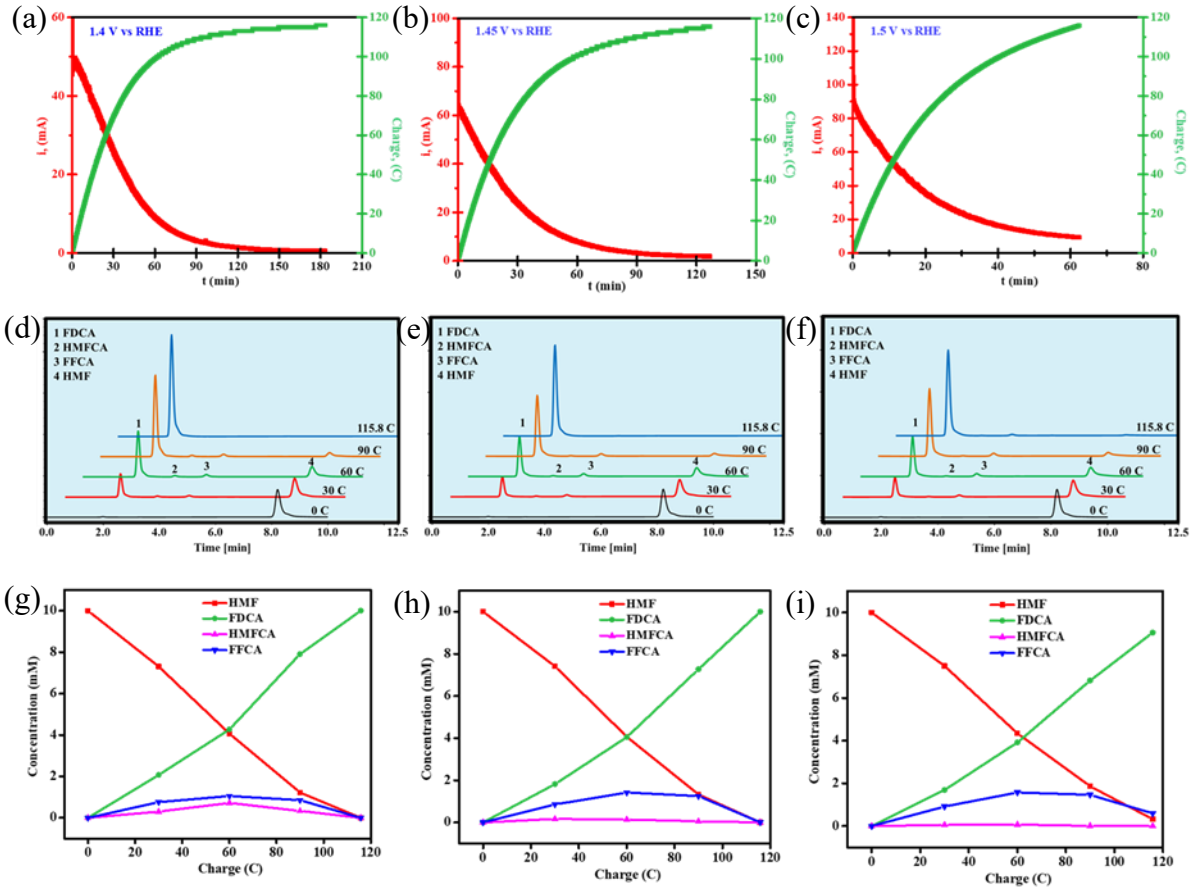

Fig. S21 (a) i - t plot illustrating the stability of $Ni_xS_y/MoS_2/MoC$ after consecutive addition of HMF (10 mM). (b) LSV obtained before and after 8 consecutive cycles towards HMF oxidation. Sweep rate: 5 mV/s

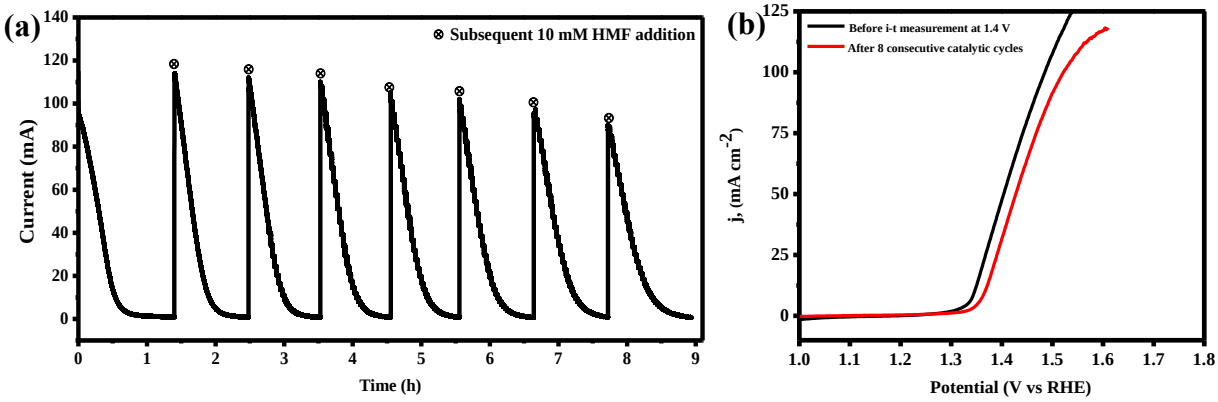

Fig. S22 Post-consecutive HMFOR (a) XRD, (b-c) FESEM image and EDX mapping image, and (d) TEM image of $Ni_xS_y/MoS_2/MoC$.

EDX spectra of $Ni_xS_y/MoS_2/MoC$ (e) before and (f) after consecutive catalytic cycles.

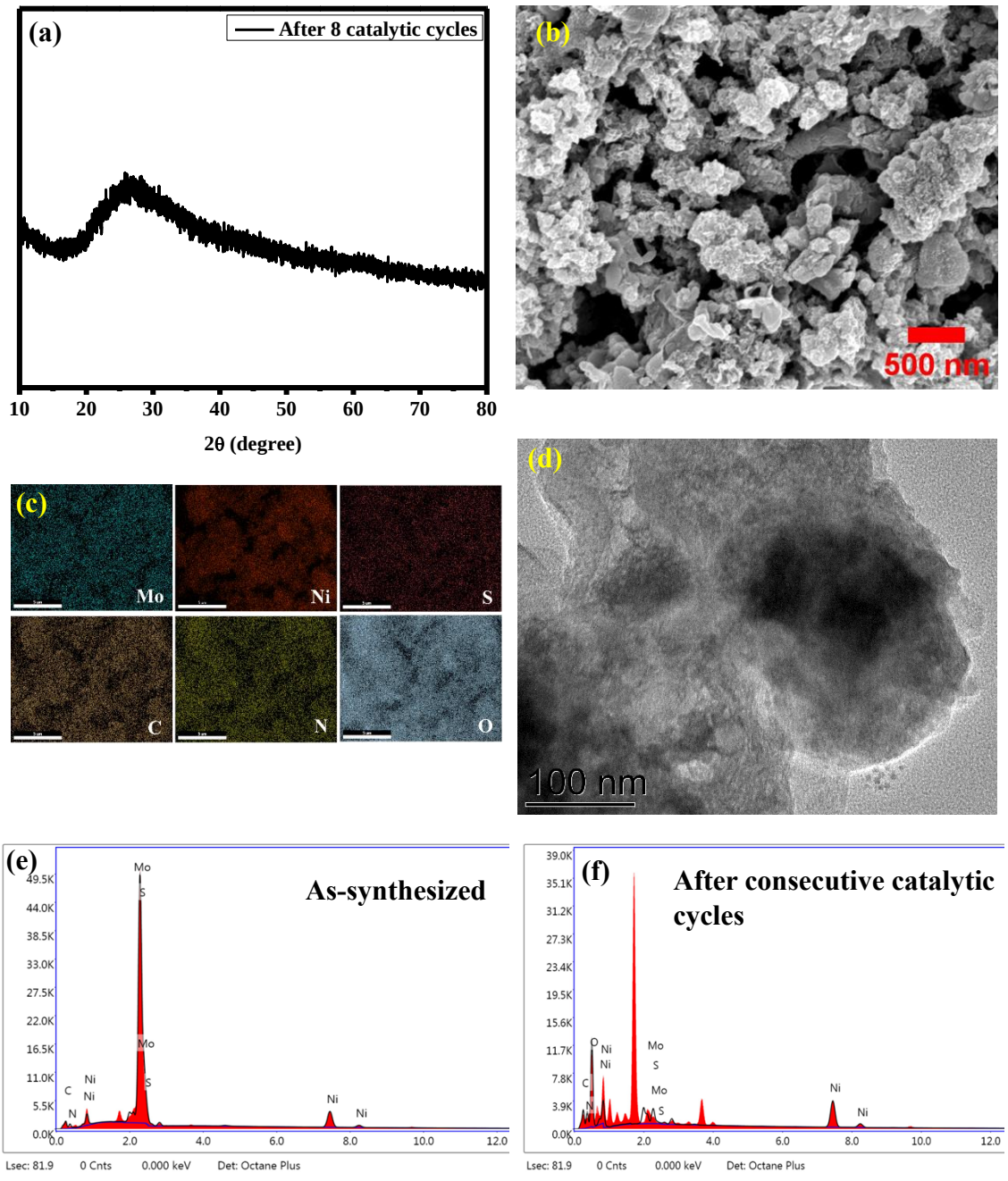

Fig. S23 XPS survey scan profile of $Ni_xS_y/MoS_2/MoC$ after HMFOR.

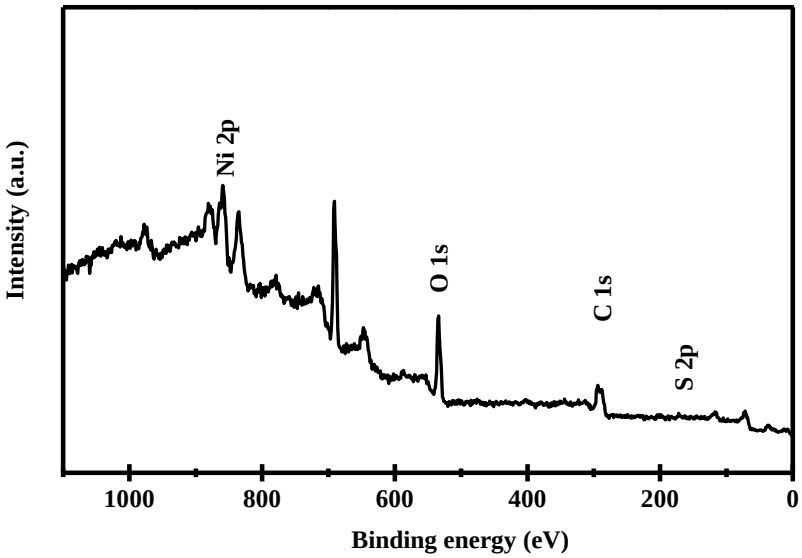

Table S1 Table summarizing the atomic % of Ni, Mo, O and S in $Ni_xS_y/MoS_2/MoC$ post catalysis.

Ni 2p3	Mo 3d	O 1s	S 2p	
8.43	13.13	13.54	23.74	As-synthesized
31.83	0.30	41.04	0	Post HMFOR

Fig. S24 Photograph showing full cell setup and the collection of electrochemically generated H_2 by water drainage method at 1.6 V.

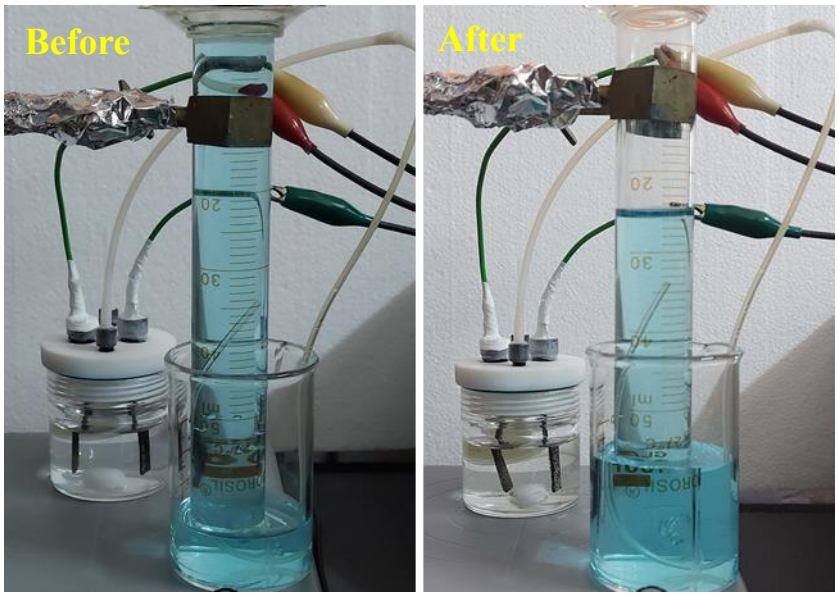

Table S2

Catalyst	Potential (RHE)	[HMF] (mM)	Amount of HMF (mmol)	Time (h)	Area (cm^2)	FE (%)	Rate of FDCA production ($mmol_{FDCA}$/ $mmol_{HMF}$/h /cm)	Ref.
$Ni_xS_y/MoS_2/MoC$	**1.4 V**	**10**	**0.2**	**1.08**	**2**	**~100**	**0.463**	**This work**
$Ni_{0.2}Mo_{0.8}N$	1.423 V	10	0.45	~4.5	--	99.3	--	2
Ni_3Fe/V_o-NiOOH	1.55 V	50	0.15	6	2	~100	0.083	3
CuH_NWs@Ce: NiH_NS	1.45 V	10	0.3	2	3	98	0.49	4
NiCoFeS-MOF	1.39 V	50	0.5	~2	1	99	0.509	5
CF-Ni MOF/Ag	1.623 V	10	0.4	2.5	--	98.6	--	6
$NiMo_3S_4$	1.414 V	10	0.2	2	--	98.4	--	7
$Mn_{0.2}NiS$	1.48 V	100	1	20 mins	1	94.2	2.854	8
NiS_x/β-$Ni(OH)_2$	1.413 V	10	0.1	3.05	1	98.3	0.32	9
NiOOH-$Cu(OH)_2$	1.4 V	5	0.075	5.2	2	93.8	0.036	10
$Ni_{0.5}Co_{2.5}O_4$	1.5 V	10	0.1	2.78	0.2	90.3	1.67	11
NiFe LDH	1.48 V	10	0.1	~3.25	--	84.4	--	12
Co_9S_8– Ni_3S_2@NSOC	1.4 V	10	0.2	2.78	1	98.6	0.356	13
CoP/Ni_2P/NiCoP @NC	1.45 V	5	0.1	5.5	1	97.6	0.177	14
$NiCo_2O_4$	1.45 V	10	0.33	~2.17	3	99	0.152	15
NiCu NTs	1.424 V	20	0.8	2	--	99	--	16

NiVCo-LDHs	1.376 V	10	0.1	1.83	3	97.8	0.534	17
Ni_xSe_y–NiFe LDH@NF	1.423 V	10	0.3	1.42	1	98.9	0.545	18
Ni, Co, Cu NPs	1.47 V	10	0.1	18	2.25	94.1	0.023	19
NiO by Co doping	1.47 V	10	0.15	4	1	94.6	0.237	20
[Ru/$Ni(OH)_2$]	1.45 V	5	0.05	0.5	3	98.5	0.65	21
Ni_3S_2-MoS_2	1.45 V	20	0.6	2.5	--	~100	--	22
S−Ni@C-600	1.437 V	10	0.15	4.5	0.5	96	0.427	23
$Ni_{0.9}$-$Cu_{0.1}(OH)_2$	1.45 V	5	0.2	2	2	91.2	0.24	24
NiSx/Ni_2P	1.46 V	10	0.15	3	1.7	95.1	0.193	25

Unit for rate of FDCA formation is h^{-1} cm^{-2}, however it is reported as $mmol_{FDCA}/mmol_{HMF}$ h^{-1} cm^{-2} for comparison purpose.

--Electrode area not available.

References

(1) M. Manikanta Kumar and C. R. Raj, *ACS Appl. Mater. Interfaces,* 2022, **14**, 15176–15186

(2) M. Sun, J. Yang, J. Huang, Y. Wang, X. Liu, Y. Qi, and L. Zhang, *Langmuir* 2023, **39**, 3762–3769.

(3) J. Liu, and S. Tao, *Adv. Sci.,* 2023, 2302641.

(4) G. Ren, B. Liu, L. Liu, M. Hu, J. Zhu, X. Xu, P. Jing, J. Wu, and J Zhang*, Inorg. Chem.* 2023, **62**, 12534–12547.

(5) Y. Feng, K. Yang, R. L. Smith, Jr, and X. Qi, *J. Mater. Chem. A*, 2023,**11**, 6375-6383.

(6) X. Pang, H. Zhao, Y. Huang, B. Luo, H. Bai, and W. Fan, *Appl. Surf. Sci.,* 2023, **608**, 155152

(7) T. Wu, Z. Xu, X. Wang, M. Luo, Y. Xia, X. Zhang, J. Li, J. Liu, J. Wang, H-. Li. Wang, and F. Huang, *Appl. Catal. B,* 2023, **323**, 122126

(8) S. Li, S. Wang, Y. Wang, J. He, K. Li, Y. Xu, M. Wang, S. Zhao, X. Li, and X. Zhong, *Adv. Funct. Mater.,* 2023, **33**, 2214488.

(9) C. Liu, X-. R. Shi, K. Yue, P. Wang, K. Zhan, X. Wang, B. Y. Xia, and Y. Yan, *Adv. Mater.* 2023, **35**, 2211177.

(10) J. Woo, B. C. Moon, U. Lee, H-. S. Oh, K. H. Chae, Y. Jun, B. K. Min, and D. K. Jee, *ACS Catal.* 2022, **12**, 4078–4091.

(11) Y. Lu, T. Liu, Y-. C. H, L, Zhou, Y. Li, W. Chen, L. Yang, B. Zhou, Y. Wu, Z. Kong, Z. Huang, Y. Li, C-. Li. Dong, S. Wang, and Y. Zou, *ACS Catal.,* 2022, **12**, 4242–4251.

(12) Y-. F. Qi, K-. Y. Wang, Y. Sun, J. Wang, and C. Wang, *ACS Sustainable Chem. Eng.* 2022, **10**, 645–654.

(13) Y. Zhang, Z. Xue, X. Zhao, B. Zhang, and T. Mu, *Green Chem.,* 2022, **24**, 1721-1731.

(14) M. Zhou, J. Chen, and Y. Li, *Catal. Sci. Technol.,* 2022,**12**, 4288-4297.

(15) Z. Zhou, Y, Xie, L. Sun, Z. Wang, W. Wang, L. Jiang, X. Tao, L. Li, X-. H. Li, and G. Zhao, *Appl. Catal. B,* 2022, **305**, 121072.

(16) L. Zheng, Y. Zhao, P. Xu, Z. Lv, X. Shi, and H. Zheng, *J. Mater. Chem. A*, 2022,**10**, 10181-10191.

(17) L. Gao, X. Wen, S. Liu, D. Qu, Y. Ma, J. Feng, Z. Zhong, H. Guan, and L. Niu, *J. Mater. Chem. A*, 2022, **10**, 21135-21141.

(18) Y. Zhong, R-. Q. Ren, J-. B. Wang, Y-. Y. Peng, Q. Li, and Y-, M. Fan, *Catal. Sci. Technol.*, 2022, **12**, 201-211.

(19) Y. Zhou, Y. Shen, and H. Li, *Appl. Catal. B*, 2022, **317**, 121776.

(20) Y. Yang, D. Xu, B. Zhang, Z. Xue, and T. Mu, *Chem. Eng. J*, 2022, **433**, 133842.

(21) X. Chai, K. Jiang, J. Wang, Z. Ren, X. Liu, L. Chen, X. Zhuang, and T. Wang, *ChemSusChem.*, 2022, **15**, e202200863.

(22) S. Yang, Y. Guo, Y. Zhao, L. Zhang, H. Shen, J. Wang, J. Li, C. Wu, W. Wang, Y. Cao, S. Zhou, Q. Zhang, and H. Zhang, S*mall* 2022, **18**, 2201306.

(23) F. Kong, and M. Wang, *ACS Appl. Energy Mater.* 2021, **4**, 1182–1188.

(24) J. Zhang, P. Yu, G. Zeng, F. Bao, Y. Yuan, and H. Huang, *J. Mater. Chem. A*, 2021, **9**, 9685-9691.

(25) B. Zhang, H. Fu, and T. Mu, *Green Chem.*, 2022, **24**, 877-884.